UCRL-JC-130610
PREPRINT

Strongly-Driven Laser Plasma Coupling

W. L. Kruer, E. M. Campbell, C. D. Decker,
S. C. Wilks, J. Moody, T. Orzechowski,
L. Powers, L. J. Suter, B. B. Afeyan, and N. Dague

This paper was prepared for submittal to the
1998 International Congress on Plasma Physics
Prague, Czech Republic
June 29 - July 3, 1998

June 25, 1998

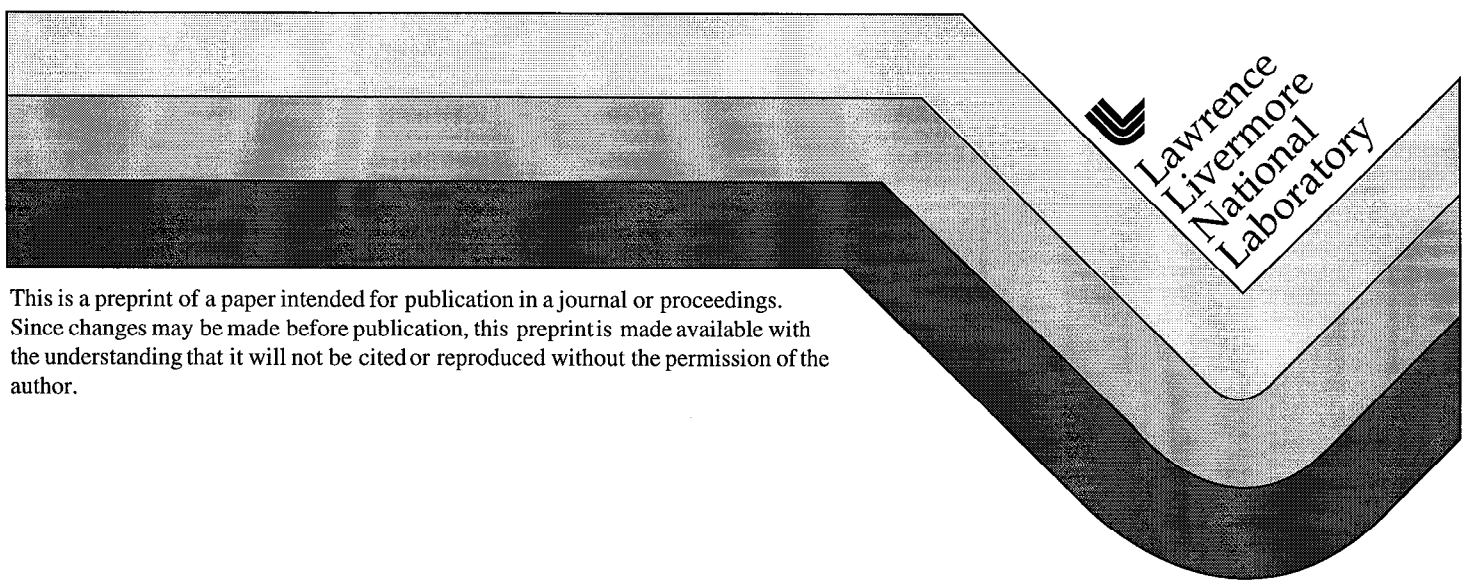

Strongly-Driven Laser Plasma Coupling

W. L. Kruer, E.M. Campbell, C.D. Decker, S.C. Wilks, J. Moody, T. Orzechowski, L. Powers, L. J. Suter
Lawrence Livermore National Laboratory, P.O. Box 808, Livermore, California 94550

B.B. Afeyan
Polymath Associates

N. Dague
Commissariat a l'Energie Atomique, Bruyeres-le-Chatel

Abstract

An improved understanding of strongly-driven laser plasma coupling is important for optimal use of the National Ignition Facility (NIF) for both inertial fusion and for a variety of advanced applications. Such applications range from high energy x-ray sources and high temperature hohlraums to fast ignition and laser radiography. We discuss a novel model for the scaling of strongly-driven stimulated Brillouin and Raman scattering. This model postulates an intensity dependent correlation length associated with spatial incoherence due to filamentation and stimulated forward scattering. We first motivate the model and then relate it to a variety of experiments. Particular attention is paid to high temperature hohlraum experiments, which exhibited low to modest stimulated Brillouin scattering even though this instability was strongly driven. We also briefly discuss the strongly nonlinear interaction physics for efficient generation of high energy electrons either by irradiating a large plasma with near quarter-critical density or by irradiating overdense targets with ultra intense laser light.

Introduction

The coupling of intense laser light with plasmas is an extremely rich and challenging topic. The coupling mechanisms[1] span the gamut from inverse bremssthralung and linear mode conversion to many nonlinear optical processes. These include stimulated Raman scattering (SRS) from electron plasma waves, stimulated Brillouin scattering (SBS) from ion sound waves, and laser beam self-focusing and filamentation. These processes depend upon laser intensity and produce effects such as changes in the efficiency and location of the absorption and generation of very energetic electrons. Depending on the application, one wishes to either minimize or maximize various nonlinear processes.

Laser plasma coupling is a very important constraint for the conventional approach to inertial fusion. Figure 1 is a schematic showing the

laser power versus energy parameter space available for target design. Hydrodynamic instabilities set a lower bound on the laser power.[2] If the power is too low, the capsule is compressed too slowly, giving time for too much hydrodynamic instability growth. Laser plasma instabilities set an upper bound on the laser power. If the power is too high, these instabilities degrade the coupling of laser energy to the target. The ongoing physics agenda for inertial fusion research is to better understand these boundaries and to learn how to extend them.

To control nonlinear plasma interactions in inertial fusion, one uses short wavelength laser light (wavelength $\leq$0.35 micron), keeps the peak laser intensity moderate ($<2 \times 10^{15}$ W/cm^2), and employs laser beam smoothing techniques such as smoothing by spectral dispersion (SSD) which introduces spatial and temporal incoherence. Furthermore, hohlraum designs are restricted to allow only a low density fill plasma (density $<0.1\ n_{cr}$, where n_{cr} is the critical density). There is considerable interest in understanding regimes in which the laser plasma coupling is more strongly driven, i.e., the above constraints are violated. This improved understanding will help determine where these constraints can be loosened, which will allow improved target designs or perhaps the use of 0.53 μm laser light.[3] In addition, there are potential new applications which exploit nonlinear effects, such as the generation of electrons with an energy in the MeV range by ultraintense laser light.

Strongly-Driven Stimulated Brillouin Scattering and a Scaling Model

Stimulated Brillouin scattering can efficiently scatter laser light and so can lead to low coupling efficiency, which is clearly undesirable. The scaling of this scattering with intensity, plasma density, and scale length is then a significant issue. Our current understanding of this scaling is poor. As an example, Fig. 2 shows the reflectivity versus intensity measured in experiments[4] with large gas-filled hohlraums on the Nova laser. Note that the SBS reflectivity, after an abrupt onset, tends to saturate with intensity. Similar results have been observed in experiments[5,6] with gas bags. Likewise there have been experiments[7,8] in which smaller hohlraums are irradiated with the Nova laser to maximize the radiation temperature. Although these smaller hohlraums are calculated to fill to densities substantially greater than $0.1\ n_{cr}$ and to have high SBS gains, small-to-modest levels of SBS were measured.

These and many other experimental results emphasize the need to develop a new scaling model. The scaling model based on the linear instability gain from heavily-damped ion waves is well-known. The reflectivity (r) then scales as

$$r \sim B \exp(kIL/\nu) \qquad (1)$$

where B is a noise level, I is the laser intensity, L is the plasma size, and ν is the ion wave damping rate. Not surprisingly, such a model does not generally predict the scaling of the measured reflectivities and is sometimes qualitatively wrong. For example, the analogous scaling model for stimulated Raman scattering predicted no dependence on ion wave damping in contrast to experiments.[9]

There has been an evolution in improvements. It is clearly important to average over a distribution of intensities, which have a well-defined distribution for a laser beam smoothed by a random phase plate. The reflectivity then onsets[10] at a significantly lower average intensity, since the more intense speckles first become unstable. Attention has also been given to determining the proper damping rate to use in the gain coefficient. One cannot in general simply use the linear Landau damping rate. The effective ion wave damping can depend on ion-ion collisions[11], long wavelength velocity modulations[12], and even on modified electron velocity distributions.[13]

A natural next step in the model evolution is to replace L with an intensity-dependent correlation length. Such a reduction in the interaction region has been suggested by research[14] on plasma-induced spatial incoherence. For example, Afeyan and Schmitt[15] have recently pointed out the importance of including not just intensity statistics but intensity-times-length statistics. The very idealized model here considered invokes a nonlinear coherence length set by laser beam filamentation. This hypothesis is motivated by research showing that spatial incoherence both suppresses[16] and nonlinearly results[17,18] from filamentation.

Let us then consider a simple scaling for very strongly driven SBS. We consider a laser beam smoothed with a random phase plate and examine SBS from damped ion waves. Our first hypothesis is that the gain is limited to an intensity-dependent coherence length set by a nonlinearly-determined speckle length. We further assume that the different coherent regions (i.e., different speckles) do not communicate. Then the reflectivity r becomes

$$r \sim \Sigma B \frac{L}{\ell_{coh}} \exp Q \qquad (2)$$

where ℓ_{coh} is a coherence length to be discussed shortly. The symbol Σ denotes a sum over the intensity distribution. The gain coefficient Q is

$$Q = \frac{\pi}{2}\frac{\ell_{coh}}{\lambda_0}\left(\frac{\omega_{pe}}{\omega_0}\right)^2\left(\frac{v_{os}}{v_e}\right)^2 / \frac{\nu_i}{\omega_i} \tag{3}$$

where λ_0 is the laser wave length, $\omega_{pe}(\omega_0)$ the electron plasma frequency (laser frequency), $v_{os}(v_e)$ the electron oscillatory velocity(thermal velocity), and $\nu_i(\omega_i)$ the ion wave damping (frequency).

The second hypothesis is that the coherence length in strongly-driven plasmas is set by laser beam filamentation. In other words, filamentation nonlinearly generates angular spread which reduces the coherence length. A beam smoothed by a random phase plate is composed of speckles. These have a radius of $f\lambda_0$ and a longitudinal coherence length of $8f^2\lambda_0$, where f is the f number of the focusing lens. Filamentation can be thought of a speckle self-focusing. It occurs when the self-focusing length is less than the longitudinal coherence (speckle) length. Filamentation generates angular spread, which reduces the effective f number. The speckles then become more narrow and have a shorter coherence length. We obtain the resulting coherence length by invoking marginal stability. The ponderomotive self-focusing length $\left(\ell_{sf}\right)$ of a small beam with radius r is estimated as

$$l_{sf} = 2r\frac{v_e}{v_{os}}\frac{\omega_0}{\omega_{pe}} \tag{4}$$

The marginal stability condition is that $\ell_{sf} = \ell_{coh}$, giving the effective f number and coherence length in the nonlinear state:

$$f = \frac{1}{4}\frac{v_e}{v_0}\frac{\omega_0}{\omega_{pe}} \tag{5}$$

$$\ell_{coh} = \frac{\lambda_0}{2}\left(\frac{v_e}{v_{os}}\right)^2\left(\frac{\omega_0}{\omega_{pes}}\right)^2 \tag{6}$$

The gain coefficient now reduces to $Q = \frac{\pi}{4} / \frac{\nu_i}{\omega_i}$, giving

$$r = \sum B\frac{n}{n_{cr}}\frac{L}{\lambda_0}\left(\frac{v_{os}}{v_o}\right)^2 \exp\left[\frac{\pi}{4} / \frac{\nu_i}{\omega_i}\right] \tag{7}$$

Note the weak scaling with density, intensity, and plasma scale length, a feature in better agreement with strongly-driven experiments. The scaling with damping is also qualitatively consistent with numerous experiments[4-6] with large plasmas, which show that the reflectivity decreases as the damping

increases. Note also that the reflectivity becomes independent of the f number of the focusing lens in this limit, since the effective f number is set nonlinearly. This has also been observed in experiments.[4]

One should not expect accurate numbers for the reflectivity from such an idealized scaling model. Quantitative results require at the very least a better understanding of the self-consistent damping and detuning, which depends on fluctuations, ion-ion collisions, plasma composition and mixing, and modified distributions. However, modest levels of reflectivity can be motivated. For example, consider a Au plasma with an electron density of 0.3 n_{cr} and an electron temperature of 5 keV. Take a noise level of 10^{-8}, a spectrum of velocity fluctuations with a mean square amplite of 5%, and note that L is set by the collisional absorption length (~200 microns). Then r~5%.

This very simple scaling model also serves to focus attention on some important issues for further study. The coherence length will depend on both spatial and temporal incoherence. Other processes[18] such as stimulated Brillouin forward scattering, scattering from background plasma modulations, and thermal filamentation will contribute to this incoherence. Likewise, the communication among speckles can depend on processes such as modified electron velocity distributions[13], which can make the ion wave frequency a function of speckle intensity. Finally, an accurate calculation of ion wave damping requires more attention to how the distribution functions evolve and how different ion species intermingle.

Strongly-Driven SRS and Two-Plasmon-Decay

To develop x-ray sources, one may aim to efficiently generate very energetic electrons. Electrons with a temperature in the 50-100 keV range can be produced by irradiating a hohlraum filled with plasma with a density near 0.25 n_{cr}. The hot electrons are produced by electron plasma waves associated with either SRS or with the two-plasmon-decay (the 2 ω_{pe} instability, where ω_{pe} is the electron plasma frequency). These hot electrons bremssthralung in the Au hohlraum walls to provide a bright source of x-rays with a temperature in the range of 50-100 keV.

Efficient generation[19] of such hot electrons was first demonstrated in early hohlraum experiments using the Shiva laser. In these experiments, up to 50% of the laser energy was inferred via hard x-ray spectra to be deposited into hot electrons with a temperature of about 50 keV. The hot electron generation was observed to correlate with the measured stimulated Raman-scattered light, and the timing was correlated with the filling[20] of the interior of the hohlraum with plasma to a density near 0.25 n_{cr}. Of course, these energetic electrons were very deleterious for inertial fusion implosions, since they preheated the capsules. Minimizing their generation led to the use of

shorter wavelength laser light. The NIF will operate at a wavelength of 0.35 micron.

However, NIF could still be used to develop an x-ray source by irradiating large plasmas near 0.25 n_{cr} in specially designed hohlraum targets. For this application, the laser could output 0.53 micron or possibly even 1.06 micron light. Given this capability and the potential application, we are motivated to further examine hot electron generation by SRS and the 2 ω_{pe} instability in large, hot plasmas. Simple estimates show that NIF will be able to create large regions (size >3 mm) of near 0.25 n_{cr} plasma with an electron temperature >4 keV.

In such hot plasmas, our one and two-dimensional PIC simulations show that the high energy electron temperatures nonlineary generated by the two different processes are quite similar close to 0.25 n_{cr}. As detailed by Simon, et al.[21], Landau damping in a hot plasma significantly restricts the plasma waves driven unstable by the 2 ω_{pe} instability. In contrast to the cold plasma case, the strongest growth occurs when the forward-directed plasma wave takes up most of the laser light momentum, i.e., $k=k_0$, where k (k_0) is the wavenumber of the plasma wave (the light wave). This plasma wave then has a phase velocity close to that of the Raman-generated plasma wave.

Recent results from 1-D PIC simulations are shown in Fig. 3. Figure 3a shows the heated electron distribution for a representative case with a plasma density of 0.23 n_{cr}, illustrating the hot electron tail which is generated. Figure 3b shows how the effective temperature of these electrons scales with intensity when the ion damping is varied by changing the ion-electron temperature ratio. For strong ion wave damping, the hot temperature is weakly dependent[22] on intensity and has a value $= mv_p^2/2$, which is about 90 keV for this density. For weaker ion wave damping, comparable temperatures are found but now with an intensity scaling similar to that proposed by Lasinski, et al.[23], for the 2 ω_{pe} instability. In principle, over 50% of the laser light can be converted into hot electrons, especially if one operates near 0.25 n_{cr} where both processes are operative.

Ultra Intense Regimes

Finally, let us briefly discuss ultra intense regimes and some related applications. Advances in laser science[24] are allowing us to access laser matter interactions with focused laser intensities up to 10^{21} W/cm^2. At such an intensity, the energy of oscillation of an electron in the laser field is about 10 MeV, and the light pressure is about 3 x 10^5 Mbars. This is clearly a new regime with strongly nonlinear and relativistic interaction physics and many potential applications.

Some of the applications require the efficient generation of electrons with energies in some appropriate range. For example, the range of a 3.5 MeV alpha particle is about equal to the range of an electron with an energy of 1 MeV. Hence, such electrons can be used as a "match" to initiate thermonuclear burn in cold, precompressed fuel. A new, more efficient approach[25] to inertial fusion may then be possible if such electrons could be efficiently generated by a short, intense laser pulse. For laser radiography applications[26], electrons with energies of order 5-10 MeV are desired. Such electrons produce x-rays via bremssthralung, which have minimum attenuation in heavy metals and so can provide high resolution radiographs.

The efficiency of hot electron generation and their energy spectra are clearly important issues. Early simulations were quite hopeful. These ideal simulations[27] using a 2-D relativistic PIC code considered a focused light beam incident onto a sharply-rising overdense plasma. Reasonably efficient absorption (30–50%) was found into hot electrons with a characteristic energy about equal to the energy of electron oscillation in the linearly-polarized laser field, i.e.,

$$\varepsilon_p = mc^2\left[\left(1 + I\lambda_\mu^2 / 2.8x10^{18}\right)^{.5} - 1\right]$$

where I is the intensity, λ_μ is the wavelength in microns, and mc^2 is the rest mass energy of an electron. The absorption was due to a combination of JxB heating (due to the oscillating pondermotive force) and not-so-resonant absorption. Although such results are a promising point of departure, more complex calculations are no doubt required to understand this extremely nonlinear coupling regime.

For one thing, in current experiments[28] with the Petawatt laser at LLNL, there is a significant prepulse which preforms a region of underdense plasma. We estimate that this underdense plasma has a scale length about equal to the focal spot diameter, which is typically 15-30 microns. In this preformed plasma, the laser beam can readily break into intense filaments which then strike the overdense plasma. Figure 4 shows contours of the laser electric field from a 2-D PIC simulation of a focused light beam incident onto a plasma. In front of an overdense plasma with a density of 3 n_{cr} is an underdense plasma which rises in density from 0.2 n_{cr} to 0.6 n_{cr} in 70 c/ω_0. Note that the laser beam breaks into intense filaments with a diameter approximately equal to the free space wavelength of the light. Although the incident peak intensity was $<10^{18}$ W/cm^2, the filamented intensity striking the overdense plasma has become about 10^{19} W/cm^2. These results are consistent with gain length estimates for relativistic filamentation.

An underdense plasma also introduces new sources of very energetic electrons. Some estimates for hot electron generation by Raman forward scattering are instructive. As a characteristic energy, we use E_p, the energy of an electron moving with the phase velocity of the associated electron plasma wave. This energy varies from greater than 10 MeV for $A=10^{-3}$ to less than an MeV for A=0.1, where $A = \omega_{pe}^2 / \gamma\omega_0^2, \gamma = \left(1 + 0.5(p_{os}/mc)^2\right)^{0.5}$, and p_{os} is the oscillating momentum in the laser field. However, the estimated efficiency is small due to the small heat capacity of the underdense plasma. To see this, assume that 20% of the electrons are heated to E_p, giving a maximum energy flux of $0.2nE_pc$, where n is the density and c the velocity of light. For 1.06 micron light with an intensity of 2×10^{22} W/cm^2, the maximum energy flux remains less than 0.5% of the incident intensity.

A clear picture of the efficiency of hot electron generation and its dependence on intensity has not yet emerged from experiments with ultra intense light. In recent experiments[29] high energy electrons were inferred via measurements of Kα emission for nominal intensities ranging from 10^{18} to 10^{20} W/cm^2. The efficiency of hot electron generation was inferred to be 20–30%. The intensity dependence of the hot electron energies was less clear. Laser beam filamentation is perhaps operative in these experiments. Meanwhile, a broad range of work continues on the coupling physics, ranging from theory and simulation of instability generation[30] by ultra intense light to 3-D PIC simulations.[31] A continuing challenge for the simulations is to do justice to the very dense collisional plasma which affects the hot electron transport out of the interaction region.

In summary, the laser plasma interaction physics is a rich and challenging topic which is very important for the efficient use of large, high power lasers. This coupling physics includes a variety of laser-driven instabilities as well as other nonlinear plasma effects. Significant progress continues to be made in learning how to control these plasma processes for inertial fusion and how to exploit them for various advanced applications.

Acknowledgments

We are grateful for discussions with H. Baldis, P. Rambo, W. Rozmus, W. Seka, and colleagues in the laser plasma program at LLNL. This invited presentation was made possible by travel support from the Institute for Laser Science and Applications directed by H. Baldis.

Work performed under the auspices of the U.S. Department of Energy by Lawrence Livermore National Laboratory under Contract W-7405-ENG-48.

References

1. Baldis, H.A., Campbell, E.M., and Kruer, W.L., 1991, in Physics of Laser Plasmas (North-Holland, Amsterdam) pp361-434, and many references therein.
2. Haan, S.W., et al., 1995, Phys. Plasmas 2, 2480.
3. Campbell, E.M., et al., 1997, Comments Plasma Phys. Cont. Fusion 18,201.
4. Fernandez, J.C. et al., 1996, Phys. Rev. E 53,2747.
5. MacGowan, B.J., et al., 1996, Phys. Plasmas 3,2029
6. Montgomery, D.S., et al., 1998, Phys. Plasmas 5,1973.
7. Orzechowski, T.J., et al., 1996, Bull. Am. Phys. Soc. 41,1390.
8. Dague, N., et al., 1998 (private communication).
9. Kirkwood, R.K., et al., 1996, Phys. Rev. Lett. 77,2706; Fernandez, J.C., et al., 1996 Phys. Rev. Lett. 77, 2702.
10. Rose, H.A. and DuBois, D.F., 1993 Phys. Plasmas 5,590.
11. Rambo, P.W., Wilks, S.C., and Kruer, W. L., 1997, Phys. Rev. Lett. 79,83.
12. Kruer, W. L., Wilks, S. C. Afeyan, B. B., and Kirkwood, R. K., 1996, Phys. Plasmas 3,382; Maximov, A., et. al., 1996 Phys. Plasmas 3,1689.
13. Afeyan, B. B., Chou, A. E., Matte, J. P., Town, R. J., and Kruer, W. L., 1998 Phys. Rev. Lett. 80, 2322.
14. Others have also discussed plasma-induced incoherence, including Rozmus, W., Hinkel, D., Williams, E., and Seka, W.
15. Schmitt, A. J. and Afeyan, B. B., 1998, Phys. Plasmas 5,503.
16. Bodner, S. E., et al., 1998, Phys. Plasmas 5,1901 and many references therein.
17. Wilks, S. C. , et al., 1994, Phys. Rev. Lett. 73, 2994: Young, P. E., et al., 1995, Phys. Plasmas 2, 2825.
18. Moody, J. D., et al., 1998, Lawrence Livermore National Laboratory UCRL-JC-129510.
19. Kruer, W. L., 1991, Phys. Plasmas B3,2356 and references therein.
20. Lindl, J. D., 1998, Inertial Confinement Fusion (Springer-Verlag, New York) pp24-26 and references therein.
21. Simon, A., et al., 1983, Phys. Fluids 26, 3107.
22. Estabrook, et al., 1980, Phys. Rev. Lett. 45, 1399.
23. Lasinski, et al., 1980, in Lawrence Livermore National Laboratory UCRL-50021-80, p3-30.
24. Perry, M. D. and Mourou, G., 1994, Science 264, 917.
25. Tabak, M., et al., 1994, Phys. Plasmas 1, 1626.
26. Perry, M. D., 1997, private communication.
27. Wilks, S. C., Kruer, W. L., Tabak, M., and Langdon, A. B., 1992, Phys. Rev. Lett. 69,1383; Wilks, S. C. and Kruer, W. L., 1997, J. Quantum Elect. 33, 1.
28. Key, M. H., et al., 1998, Phys. Plasmas 5, 1960.
29. Wharton, K., et al., Phys. Rev. Lett. (in press).
30. Adam, J. C., et al., 1997, Phys. Rev. Lett. 78, 4765 and references therein.
31. Pukhov, A. and Meyer-ter-Vehn, J., 1998, Phys. Plasmas 5, 1880 and references therein.

Figure Captions

Figure 1: A schematic illustrating the laser power versus energy parameter space for ignition target design.

Figure 2: The SBS reflectivity into the interaction beam cone from a gas-filled hohlraums versus laser intensity. A pronounced dip in the reflectivity does not occur if the near back scatter is included.

Figure 3: a) the heated electron distribution from a 1-D simulation using a particle code illustrating a tail of high energy electrons; b) the effective temperature characterizing the high energy electrons versus laser intensity.

Figure 4: Contours of laser electric field from a 2-D simulation of a focused laser beam incident onto a plasma with both underdense and overdense regions.

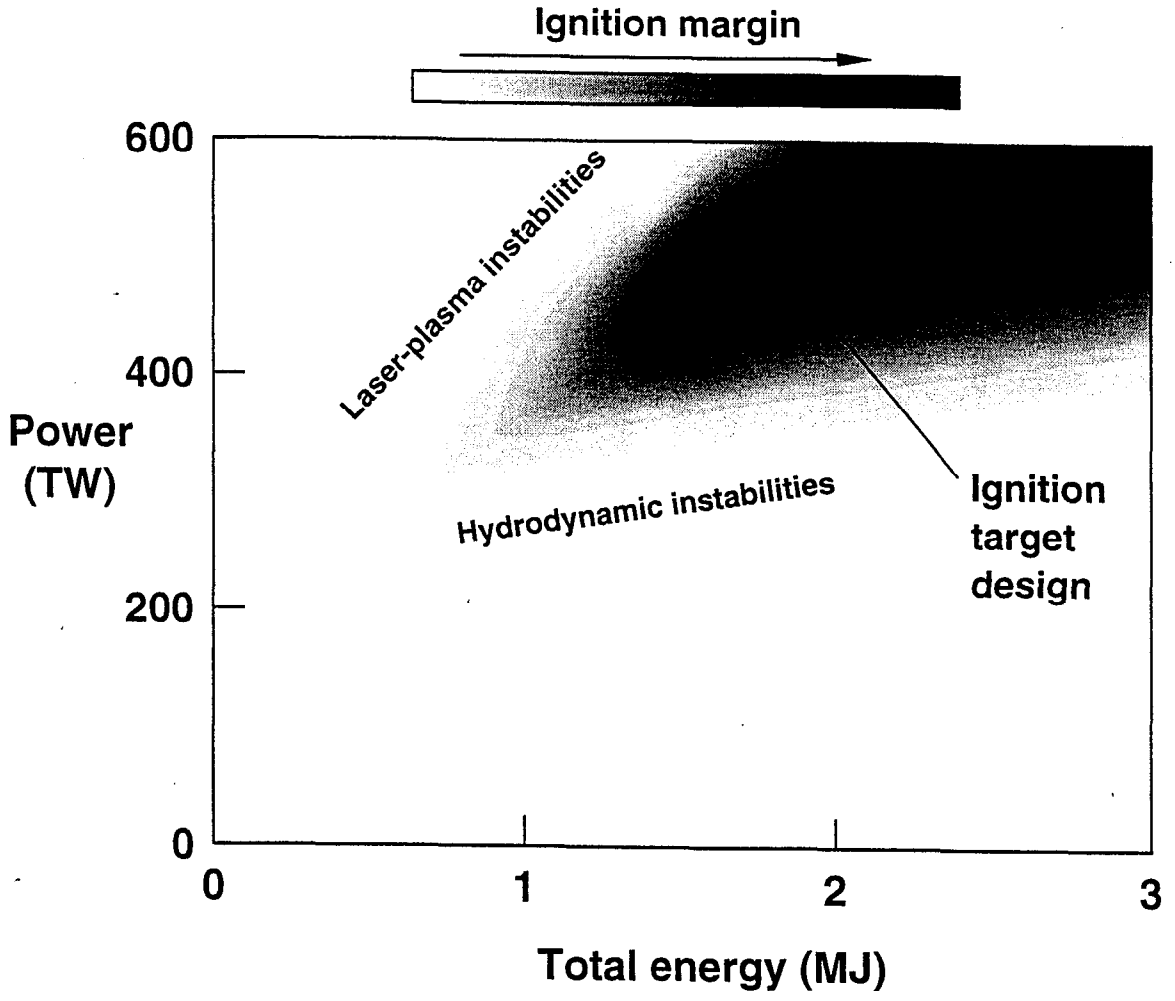
Ignition margin
600
400
200
0
Power
(TW)
Laser-plasma instabilities
Hydrodynamic instabilities
Ignition
target
design
0
1
2
3
Total energy (MJ)

Figure 1.

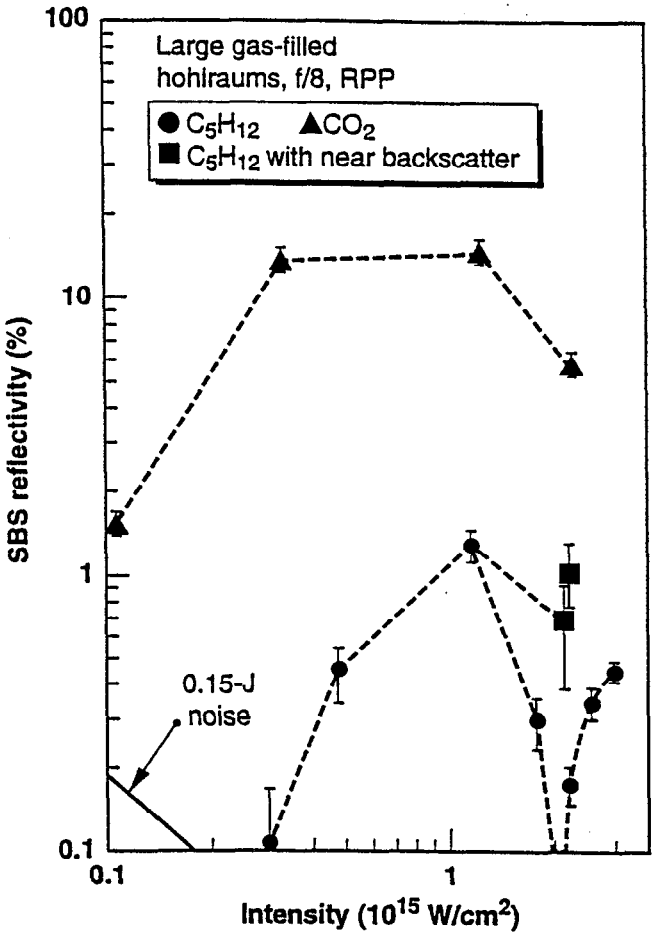
100
10
1
0.1
0.1
1
SBS reflectivity (%)
Intensity (10^{15} W/cm^2)
Large gas-filled
hohlraums, f/8, RPP
C_5H_{12} CO_2
C_5H_{12} with near backscatter
0.15-J
noise

Figure 2.

Figure 3.

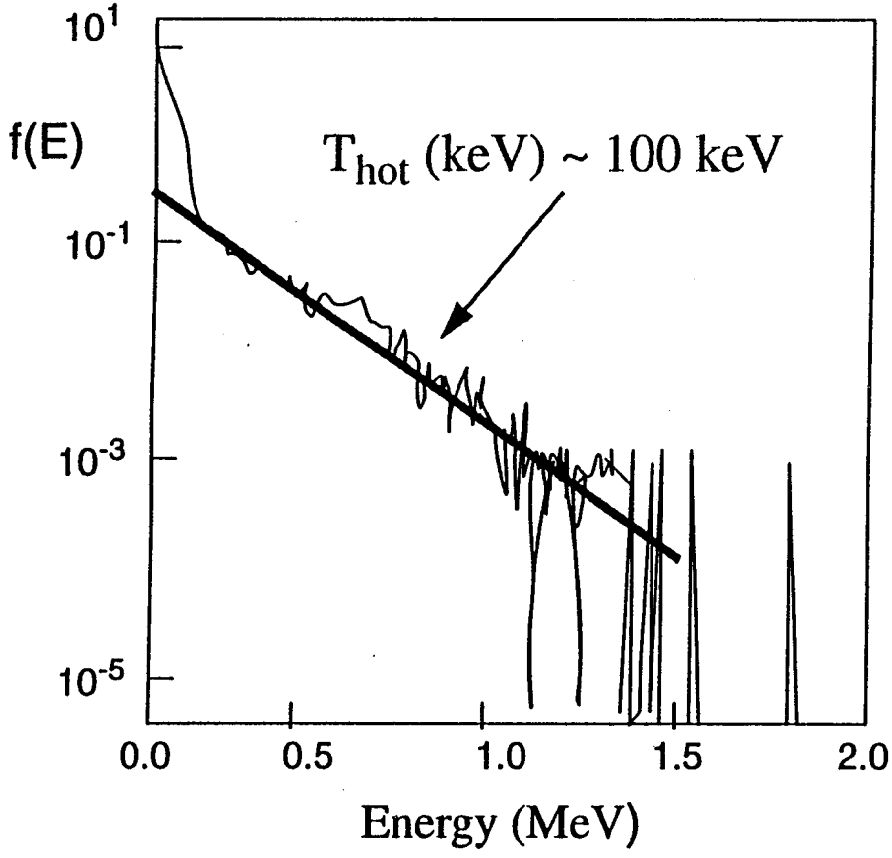
10^1
f(E)
10^{-1}
10^{-3}
10^{-5}
T_{hot} (keV) ~ 100 keV
0.0
0.5
1.0
1.5
2.0
Energy (MeV)

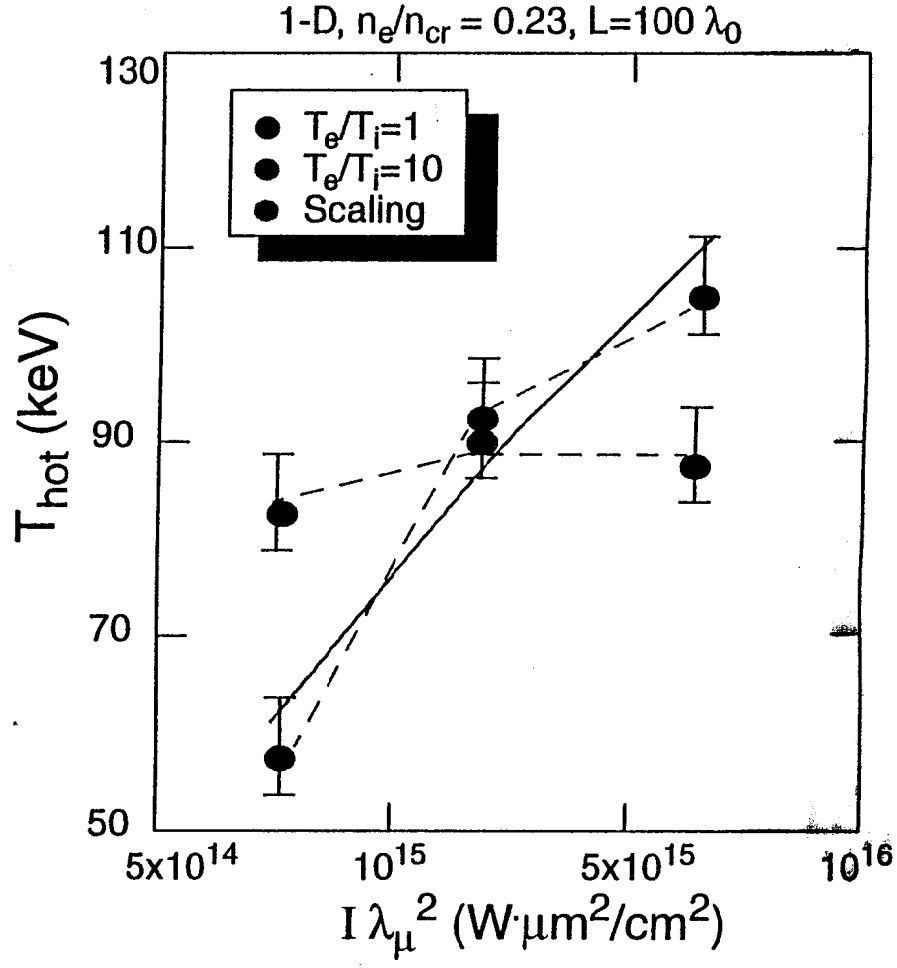
1-D, n_e/n_{cr} = 0.23, L=100 λ_0
T_e/T_i=1
T_e/T_i=10
Scaling
130
110
90
70
50
T_{hot} (keV)
$5x10^{14}$
10^{15}
$5x10^{15}$
10^{16}
$I\lambda_\mu{}^2$ (W·μm²/cm²)

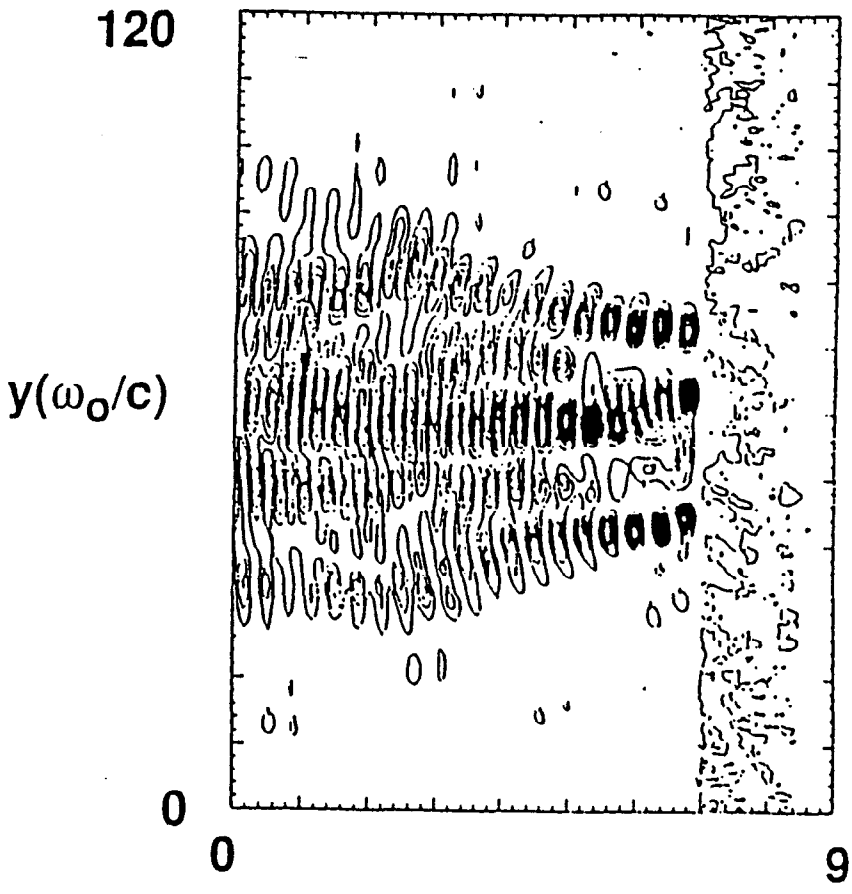
120
y(ω_o/c)
0
0
90
x(ω_o/c)
underdense plasma
(0.2-0.6 n_cr)
overdense plasma
(3n_cr)

Figure 4.